Available online at www.sciencedirect.com
SCIENCE DIRECT®
Biochemical and Biophysical Research Communications 326 (2005) 402–409
BBRC
www.elsevier.com/locate/ybbrc

Constitutively active PDX1 induced efficient insulin production in adult murine liver

Junta Imai[a,b], Hideki Katagiri[b,*], Tetsuya Yamada[a], Yasushi Ishigaki[a], Takehide Ogihara[b], Kenji Uno[a,b], Yutaka Hasegawa[a,b], Junhong Gao[a,b], Hisamitsu Ishihara[a], Hironobu Sasano[c], Hiroyuki Mizuguchi[d], Tomoichiro Asano[e], Yoshitomo Oka[a]

[a] *Division of Molecular Metabolism and Diabetes, Tohoku University Graduate School of Medicine, Japan*
[b] *Division of Advanced Therapeutics for Metabolic Diseases, Center for Translational and Advanced Animal Research, Tohoku University Graduate School of Medicine, Japan*
[c] *Division of Anatomic Pathology, Tohoku University Graduate School of Medicine, Sendai 980-8575, Japan*
[d] *Division of Cellular and Gene Therapy Products, National Institute of Health Science, Tokyo, Japan*
[e] *Department of Physiological Chemistry and Metabolism, University of Tokyo, Tokyo 113-8655, Japan*

Received 21 October 2004
Available online 19 November 2004

Abstract

To generate insulin-producing cells in the liver, recombinant adenovirus containing a constitutively active mutant of PDX1 (PDX1-VP16), designed to activate target genes without the need for protein partners, was prepared and administered intravenously to streptozotocin (STZ)-treated diabetic mice. The effects were compared with those of administering wild-type PDX1 (wt-PDX1) adenovirus. Administration of these adenoviruses at 2×10^8 pfu induced similar levels of PDX1 protein expression in the liver. While wt-PDX1 expression exerted small effects on blood glucose levels, treatment with PDX1-VP16 adenovirus efficiently induced insulin production in hepatocytes, resulting in reversal of STZ-induced hyperglycemia. The effects were sustained through day 40 when exogenous PDX1-VP16 protein expression was undetectable in the liver. Endogenous PDX1 protein came to be expressed in the liver, which is likely to be the mechanism underlying the sustained effects. On the other hand, albumin and transferrin expressions were observed in insulin-producing cells in the liver, suggesting preservation of hepatocytic functions. Thus, transient expression of an active mutant of PDX1 in the liver induced sustained PDX1 and insulin expressions without loss of hepatocytic function.

Keywords: Insulin; PDX1; Gene therapy; Diabetes; Adenovirus; Transdifferentiation

Type 1 diabetes mellitus is characterized by progressive loss of pancreatic β cells, leading to a lifelong dependency on insulin treatments. Recently, marked advances have been made in transplanting pancreatic islets from human cadavers into type 1 diabetics [1]. However, immune rejection and donor supply are still major challenges in islet cell transplantation. In this context, generation of insulin-producing cells by somatic gene therapy may represent a viable alternative for the treatment for diabetes.

The liver is a possible target organ for generation of insulin-producing cells. Pancreatic and hepatic tissues both express several transcription factors such as HNF1α and C/EBPβ. In addition, these tissues also have similar glucose sensing machinery consisting of the GLUT2 glucose transporter and glucokinase. Furthermore, during embryogenesis, the liver and the ventral pancreas appear to arise from the same cell

* Corresponding author. Fax: +81 22 717 8228.
E-mail address: katagiri-tky@umin.ac.jp (H. Katagiri).

0006-291X/$ - see front matter © 2004 Elsevier Inc. All rights reserved.
doi:10.1016/j.bbrc.2004.11.047

population located within the embryonic endoderm [2]. The gene most likely to be responsible for the difference between the liver and pancreas is pancreatic and duodenal homeobox gene 1 (PDX1), also known as IDX1/IPF1/STF1. PDX1 is expressed in pancreatic buds in the endoderm prior to morphological development of the pancreas [3,4] and has been shown to play a fundamental role in regulating pancreatic development. Gene disruption of PDX1 has been shown to inhibit pancreatic bud maturation and outgrowth, resulting in complete absence of the pancreas [5]. In addition, conditional inactivation of PDX1 in insulin-producing cells results in a progressive loss of β cells, suggesting PDX1 to play an essential role in maintaining β cells [6].

Therefore, to generate insulin-producing cells, several groups have overexpressed PDX1 in various sites [7–11]. Adenovirus-mediated transfer of the PDX1 gene reportedly ameliorates streptozotocin (STZ)-induced hyperglycemia in a short time (within 10 days) [7] as well as for longer periods [12] via production of insulin in the liver. However, helper-dependent adenovirus (HDAD)-mediated PDX1 gene transfer into the liver reportedly results in severe hepatitis and functional failure due to production of pancreatic exocrine enzymes [10]. In addition, transgenic mice overexpressing PDX1 in the liver also develop liver failure [11].

PDX1 has been shown to activate target genes by association with several co-factors such as PBX [13] and the expressions of these protein partners are absent in the liver. To produce a version of PDX1 that would activate target genes without the need for protein partners, the VP16 activation domain from herpes simplex virus was fused to the C-terminus of PDX1 (PDX1-VP16). In PDX1-VP16 transgenic *Xenopus* tadpoles, part or all of the liver is converted to pancreatic tissue, while hepatic differentiation products are lost from the regions converted to pancreas [14].

Therefore, in the present study, we prepared PDX1-VP16 adenovirus and compared the effects of PDX1-VP16 expression with those of wt-PDX1 in the adult murine liver in vivo. These recombinant adenoviruses were administered at a titer of 2×10^8 pfu, which is one to two orders of magnitude lower than those used in previous reports [7,12]. Herein we demonstrate PDX1-VP16 gene transduction to induce hepatocytic production of insulin, but not glucagon or amylase, more efficiently than wt-PDX1, resulting in reversal of STZ-induced hyperglycemia. We found that PDX1-VP16 gene therapy induced endogenous PDX1 expression in the liver, and hence sustained expression of insulin. In contrast to transgenic tadpole experiments, the conversion was partial and liver-specific gene expressions including those of albumin and transferrin were maintained in insulin-producing cells.

Materials and methods

Recombinant adenoviruses. Murine PDX1 cDNA was cloned from a MIN6 cDNA library by PCR. Using PCR, the *ClaI* site was added to murine PDX1 cDNA, which was digested with *ClaI* and subcloned into VP16-N (kind gift from Dr. H. Kanamori) as described [14]. Recombinant adenoviruses containing wt-PDX1 and PDX1-VP16 cDNA were prepared as reported previously [15–17]. LacZ adenovirus was used as a control [18].

Animals. Male C57BL/6N mice were purchased from Clea (Tokyo, Japan), housed in an air-conditioned environment, with a 12-h light-dark cycle, and fed a regular unrestricted diet. Diabetes was induced by intraperitoneal injection of 160–170 mg/kg STZ (Sigma St. Louis, MO) in citrate buffer at 5–6 weeks of age. Blood glucose was determined after a 10 h fast at 6 days after STZ injection; mice with fasting glucose levels of 300–600 mg/dl were used for the experiments. The mice were treated with 2×10^8 plaque-forming units of recombinant adenovirus by systemic injection into the tail vein and killed 40 days after adenovirus injection. Serum insulin concentrations were measured using a rat insulin ELISA Kit Ultra Sensitive (Morinaga, Tokyo, Japan).

Oral glucose tolerance tests. Oral glucose tolerance tests were performed 40 days after adenovirus infusion. Serum glucose levels were determined before, and 15, 30, 60, 90, and 120 min after, administration of oral glucose (1 g/kg body weight).

Immunoblotting. Liver samples were homogenized in buffer (100 mM Tris, pH 8.5, 250 mM NaCl, 1% BP-40, and 1 mM EDTA). Tissue homogenates were centrifuged at 14,000*g* for 10 min at 4 °C. Supernatants including tissue protein extracts (180 μg total protein) were then boiled in Laemmli buffer containing 10 mM dithiothreitol. Aliquots of proteins (15 μg) were subjected to SDS–PAGE. Immunoblot analyses were performed using ECL plus a Western Blotting Detection System Kit (Amersham Buckinghamshire, UK). Antibodies to PDX1 (A-17, Santa Cruz Biotechnology, Santa Cruz, CA) and HSV-1 VP16 (vA-19, Santa Cruz Biotechnology) were commercially obtained.

Immunohistochemistry. Livers of mice were excised 40 days after adenoviral treatment and fixed overnight in 10% paraformaldehyde. Fixed tissues were processed for paraffin embedding and 3 μm sections were prepared. For immunohistochemistry, the streptavidin–biotin (SAB) method was performed using a Histofine SAB-PO kit (Nichirei, Tokyo, Japan) for insulin, glucagon, and amylase, and a MAX-PO kit (Nichirei) for somatostatin, and an EnVision kit/HRP (DAKO, Glostrup, Denmark) for pancreatic polypeptide. Slides were deparaffinized, and then were either autoclaved in citrate buffer for antigen retrieval before being incubated in blocking solution (for amylase, somatostatin, and pancreatic polypeptide detection), or immediately exposed to the blocking solution (for insulin and glucagon detection). For insulin detection, sections were incubated for 18 h at 4 °C with monoclonal antibody against human insulin (Sigma) diluted 1:1000 in PBS. For detection of glucagon, sections were incubated for 18 h at 4 °C with antiserum raised against human glucagon (DAKO) diluted 1:3000 in PBS. For detection of somatostatin, sections were incubated overnight at 4 °C with rat anti-somatostatin monoclonal antibody (Chemicon, Temecula, CA) diluted 1:100 in PBS. For detection of pancreatic polypeptide, sections were incubated overnight at 4 °C with antiserum raised against rat pancreatic polypeptide (LINCO, St. Charles, MO) diluted 1:100 in PBS. For detection of amylase, sections were incubated for 18 h at 4 °C with antiserum raised against the C-terminus of human amylase (Santa Cruz Biotechnology) diluted 1:1000 in PBS. Slides were then incubated with the biotinylated IgG for 1 h and next with peroxidase-conjugated streptavidin for 30 min at room temperature. Finally, immunoreactivity was visualized by incubation with a substrate solution containing 3,3′-diaminobenzidine tetrahydrochloride (DAB).

Fluorescent immunocytochemistry. The 3 μm sections of paraffin-embedded liver were processed as follows. For double staining of

insulin and transferrin or albumin, the sections were incubated overnight with antibodies against insulin and transferrin (goat polyclonal; Santa Cruz Biotechnology) or albumin (rabbit polyclonal; Biogenesis, Kingston, New Hampshire) at 4 °C. Antibodies against insulin, transferrin, and albumin were diluted 1:1000, 1:5000, and 1:5000, respectively, in PBS. For double staining of insulin and transferrin, the sections were then incubated for 1 h at room temperature in a mixture of TRITC-conjugated sheep anti-mouse IgG and FITC-conjugated donkey anti-goat IgG (Jackson Immuno Research, West Grove, PA) diluted 1:1000 in PBS. For double staining of insulin and albumin, the sections were incubated in a mixture of Alexa Fluor 488 goat anti-mose IgG (Molecular Probes, Eugene, OR) and Alexa Fluor 546 goat anti-rabbit IgG diluted 1:1000 in PBS. Sections were observed under a fluorescence microscope (Leica DM RXA, Leica Microsystems, Wetzlar, Germany). The image was analyzed with a Q-fluoro analyzing system (Leica).

Results

To express a PDX1 mutant, in the liver, which is constitutively active without association with protein partners, we prepared a recombinant adenovirus encoding the VP16 activation domain from herpes simplex virus [19,20] fused to the C-terminus of murine PDX1 (PDX1-VP16). For comparison, we also prepared recombinant adenoviruses encoding the wild-type PDX1 (wt-PDX1) and LacZ. These recombinant adenoviruses, at 2×10^8 pfu, were injected intravenously 6 days after STZ administration, when hyperglycemia had already developed; blood glucose levels after a 10 h fast were approximately 400 mg/dl (Fig. 1B). Mice given the LacZ adenovirus were used as controls (LacZ-mice). Systemic infusion of recombinant adenoviruses into mice through the tail vein caused transgene expression primarily in the liver, with no detectable expression in peripheral tissues such as muscle, fat, kidney or brain (data not shown), as reported previously [21].

As shown in Fig. 1A, immunoblotting of hepatic lysates on day 3 after adenoviral administration with anti-PDX1 antibody revealed that ectopic expression of wt-PDX1 or PDX1-VP16 was obtained in the liver. Administration of recombinant adenoviruses at the same titer induced similar levels of PDX1 protein expression.

We next examined the effects of treatment with these adenoviruses on STZ-induced hyperglycemia (Fig. 1B). Administration of wt-PDX1 adenovirus did not significantly decrease fasting blood glucose levels through day 20. Although, interestingly, fasting blood glucose levels were slightly but significantly decreased after day 30 as compared with those in STZ-treated LacZ-mice, administration of wt-PDX1 adenovirus at such a low titer exerted only very small effects in terms of reversal of hyperglycemia.

In contrast, administration of PDX1-VP16 adenovirus more effectively reversed STZ-induced hyperglycemia (Fig. 1B). Hepatic expression of PDX1-VP16 induced significant, profound decreases in fasting blood glucose levels. Although fasting blood glucose levels rose slightly between day 10 and day 15, the therapeutic effects were sustained throughout the experiments. As shown in Table 1, some variation in results was observed. Thirteen percent of PDX1-VP16-mice exhibited almost no decrease in blood glucose levels, although the proportion of these mice was significantly lower than that of wt-PDX1-mice. In contrast, in 27% of PDX1-VP16-mice, fasting blood glucose levels were lower than 200 mg/dl. No such normalization of glucose levels was obtained by wt-PDX1 adenovirus administration (Table 1). Thus, PDX1-VP16 expression in the liver more effectively lowered blood glucose levels and these effects persisted even after adenoviral-mediated gene expression had declined.

To examine the mechanism whereby administration of PDX1-VP16 adenovirus efficiently and persistently lowered blood glucose levels in STZ-treated mice, liver sections from these mice on day 40 after adenoviral administration were immunostained with anti-insulin antibody (Fig. 1C). No insulin staining was detectable in the livers of LacZ-mice. In wt-PDX1-mice, very faint staining with anti-insulin antibody was detected in the liver. In contrast, in PDX1-VP16 mice, strong insulin staining was detected in the cytoplasm of hepatocytes in scattered portions of the liver. The insulin positive cells were seen mostly around vessels. The scant residual insulin-positive cells in the pancreas did not differ significantly among these mice (data not shown). Thus, insulin secretion from hepatocytes is likely to contribute to lowering blood glucose levels in PDX1-VP16-mice.

To confirm that the hepatocytes were secreting insulin, serum levels of immunoreactive insulin in these mice on day 40 after adenoviral administration were measured. In LacZ-mice, STZ treatment induced severe insulinopenia: fasting serum insulin levels were less than 40 pg/ml (Fig. 1D), resulting in severe hyperglycemia. Adenoviral administration of the wt-PDX1 gene slightly increased serum insulin levels. In contrast, PDX1-VP16 adenoviral administration resulted in a substantial increase in serum insulin levels, i.e., more than 6-fold (Fig. 1D). On the other hand, fasting serum insulin levels in the control C57Bl/6N mice of the same age, without STZ treatment, were 340.7 ± 29.9 pg/ml ($n = 6$). Thus, hepatic PDX1-VP16 expression improved fasting serum insulin levels to approximately two-thirds those in normal mice. These data suggest that transient PDX1-VP16 expression in the liver exerted sustained and stronger effects in terms of production and secretion of insulin as compared with wt-PDX1 expression, resulting in the reversal of STZ-induced hyperglycemia.

Oral glucose tolerance tests were performed using LacZ-mice, wt-PDX1-mice, and PDX1-VP16-mice on day 40 (Fig. 2A). STZ-treated LacZ-mice exhibited hyperglycemia: more than 450 mg/dl throughout the

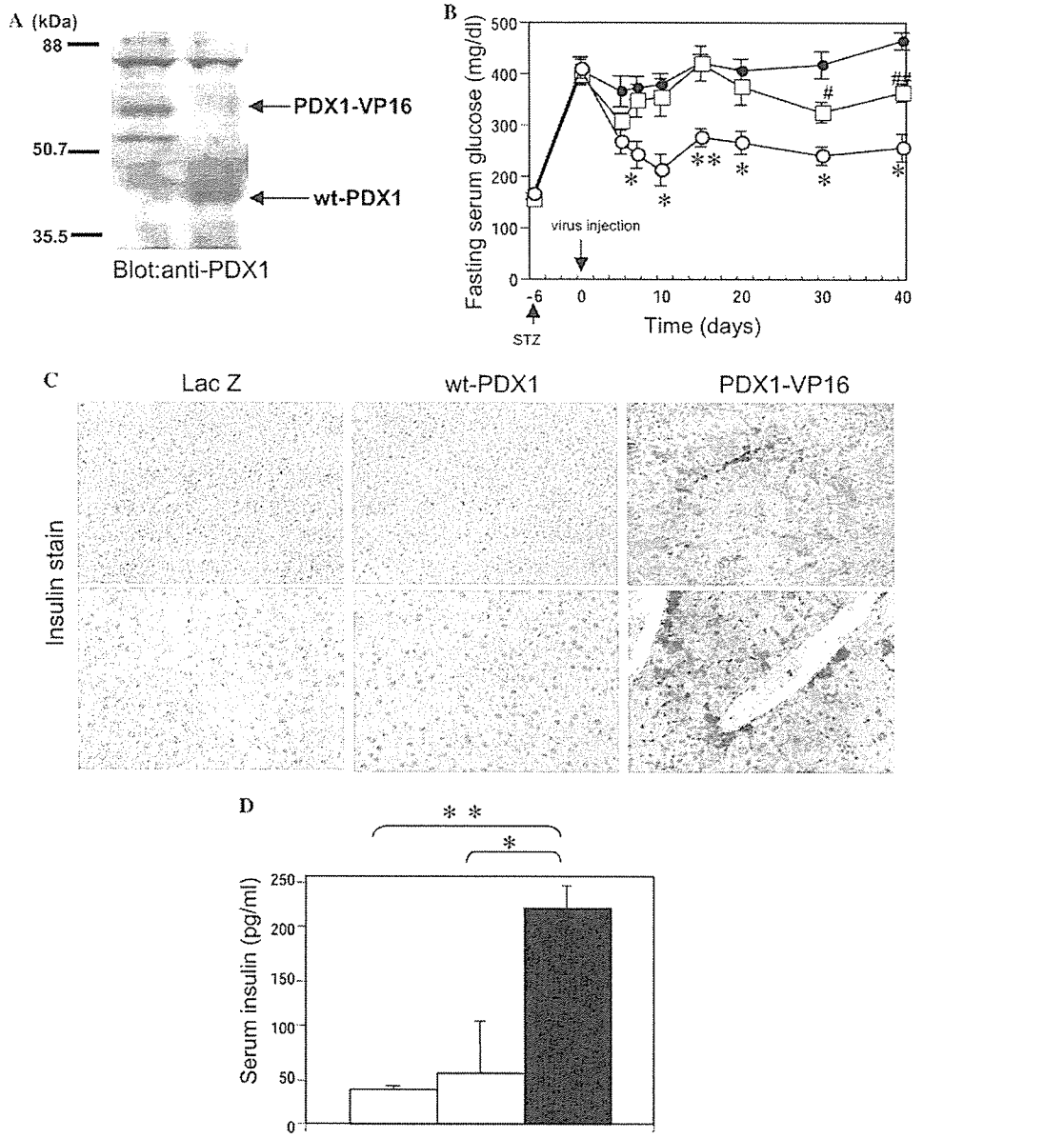

Fig. 1. Effects of wt-PDX1 and PDX1-VP16 adenoviral gene therapy on STZ-induced diabetic mice. (A) Liver lysates from STZ-mice infused with 2×10^8 pfu/body of adenovirus containing wt-PDX1 (left lane) or PDX1-VP16 (right lane) were immunoblotted with anti-PDX1 antibody. (B) Fasting blood glucose levels of STZ-mice treated with LacZ adenovirus (closed circle; $n = 13$), wt-PDX1 adenovirus (open square; $n = 8$) or PDX1-VP16 adenovirus (open circle; $n = 15$). Amount of injected adenoviruses was 2×10^8pfu/body in all experiments. (C) Liver sections from LacZ-mice (left panels), wt-PDX1-mice (middle panels), and PDX1-VP16-mice (right panels) on day 40 after adenoviral treatment were immunostained with anti-insulin antibody. Original magnification 100× (upper panels) and 200× (lower panels). (D) Fasting serum insulin levels 40 days after adenoviral treatment with LacZ (open bar; $n = 7$), wt-PDX1 (gray bar; $n = 8$), or PDX1-VP16 (black bar; $n = 7$) adenovirus. Data are presented as means ± SEM. $^*P < 0.05$, $^{**}P < 0.01$ versus wt-PDX1, $^{\#}p < 0.05$, and $^{\#\#}p < 0.01$ versus LacZ, assessed by unpaired t test.

tests. In PDX1-VP16-mice, glucose levels throughout the tests were significantly lower than those in wt-PDX1-mice. The blood glucose levels peaked at 30 min after glucose load and thereafter tended to fall, although the reversal was incomplete at 120 min. These findings suggest that, in PDX1-VP16-mice, glucose-responsive insulin secretion from the liver is involved in lowering post-prandial blood glucose levels but is not enough to rapidly reverse a rise in blood glucose levels after a glucose load, in contrast to that from the pancreas by β cells.

Using HDAD, PDX1 expression in the liver reportedly induces expression of exocrine enzymes in insulin-producing cells in the liver and causes severe hepatitis. It has also been reported that, in transgenic mice expressing PDX1 ectopically in the liver, not only insulin but

Table 1
Distribution of blood glucose levels in each treatment group

Blood glucose (mg/dl)	100–200	200–300	300–400	400–500	500–600
LacZ (%)	0	0	8	69	23
wt-PDX1 (%)	0	12	50	38	0
PDX1-VP16 (%)	27	47	13	13	0

Blood glucose levels were determined 40 days after each adenoviral treatment. Blood glucose levels of mice before the adenoviral treatment (6 days after STZ injection) were all above 300 mg/dl. (Lac Z; $n = 13$, wt-PDX1; $n = 8$, and PDX1-VP16; $n = 15$.)

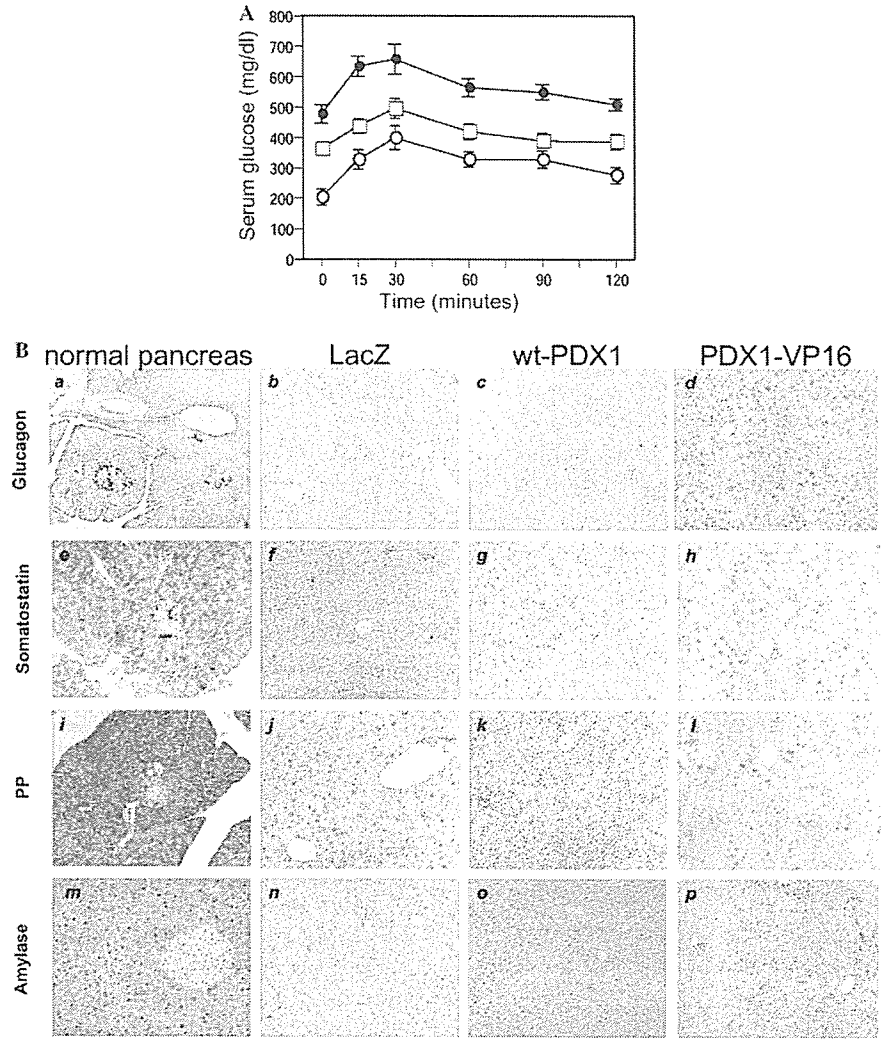

Fig. 2. Effects of wt-PDX1 and PDX1-VP16 adenoviral gene therapy on blood glucose levels after a glucose load, and glucagon, somatostatin, pancreatic polypeptide, and amylase expressions. (A) Blood glucose levels during oral glucose tolerance testing (1 g/kg body weight) in LacZ-mice (closed circle; $n = 7$), wt-PDX1-mice (open square; $n = 8$), and PDX1-VP16-mice (open circle; $n = 7$) on day 40 after adenovirus administration. Data are presented as means ± SEM. (B) immunohistochemical staining of livers from LacZ-mice (b,f,j,n), wt-PDX1-mice (c,g,k,o), and PDX1-VP16-mice (d,h,l,p) with glucagon (b–d), somatostatin (f–h), pancreatic polypeptide (j–l) or amylase (n–p) antibody. Sections of normal pancreas were used as positive controls for each staining procedure (a,e,i,m). Original magnification 100×.

also other endocrine hormones as well as pancreatic exocrine genes are expressed, resulting in dysmorphogenesis and hepatic failure [10]. In contrast, in the present study, adenovirus-mediated transduction of the wt-PDX1 or the PDX1-VP16 gene into the liver did not induce lobe structural abnormalities or substantial infiltration of inflammatory cells (Fig. 2B). Furthermore, using immunohistochemistry, no immunoreactivity against glucagon

or somatostatin was detected in livers from wt-PDX1-mice and PDX1-VP16-mice. In addition, in these livers there was no detectable production of amylase, a pancreatic exocrine enzyme (Fig. 2B), which may explain the normal morphogenesis in our experimental animals. On the other hand, pancreatic polypeptide was expressed in livers from PDX1-VP16-mice, and in those from wt-PDX1-mice though to a lesser extent. These results demonstrate that transient expression of PDX1-VP16 alters the character of hepatocytes to preferentially produce insulin and pancreatic polypeptide, but not other endocrine hormones or exocrine enzymes.

Adenoviral gene transfer induced gene expression for 1 week but, after 2 weeks, this expression reportedly disappeared [22]. However, in the present study, the blood glucose lowering effects and hepatic insulin expression persisted for at least 40 days. Therefore, the time course of PDX1 protein expression levels was examined. As shown in Fig. 3A, immunoblotting using anti-VP16 activation domain antibody revealed PDX1-VP16 protein to be expressed on day 3 but expression was markedly decreased on day 7, and undetectable on day 21. Thus, even after disappearance of VP16-PDX1 expression, hepatocytes expressed insulin, resulting in lowering of blood glucose levels. Interestingly, immunoblotting using anti-PDX1 antibody showed that endogenous PDX1 protein, which had the same molecular weight as wt-PDX1, came to be expressed on day 21. Thus, transient expression of PDX1-VP16 endowed hepatocytes with certain pancreatic β cell features and endogenous PDX1 expression is likely to maintain the insulin-producing function of these cells.

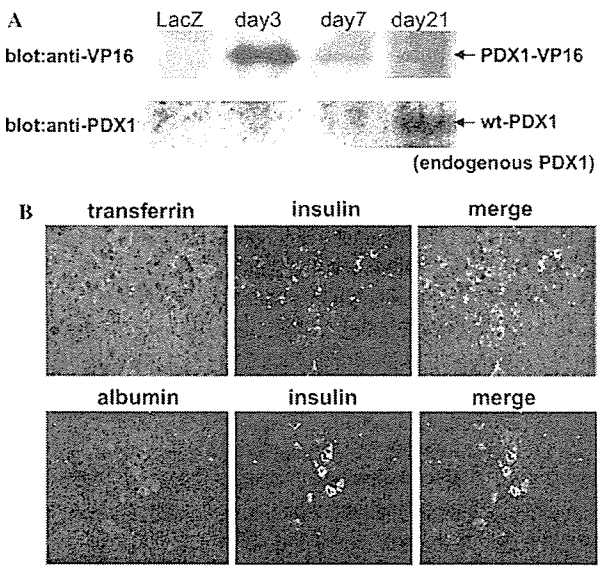

Fig. 3. Treatment with PDX1-VP16 adenovirus induced persistent expression of endogenous PDX1 but albumin and transferrin were co-expressed in insulin-expressing cells. (A) Liver lysates from PDX1-VP16 mice at different time points after adenoviral treatment were immunoblotted with anti-VP16 (upper panel) or anti-PDX1 (lower panel) antibody. (B) Liver sections from PDX1-VP16 mice on day 40 were double-immunostained with insulin (middle panels) and transferrin (upper-left panels) or albumin (lower-left panels) antibodies. Right panels represent the merged images.

To determine whether the insulin-producing cells in the liver had completely transdifferentiated and lost their hepatocytic character, liver sections from PDX1-VP16 mice on day 40 were immunostained with insulin and transferrin (upper panels in Fig. 3B) or albumin (lower panels in Fig. 3B). Fluorescence immunohistochemistry revealed that insulin-producing cells in the liver also expressed transferrin and albumin. Expression levels of these liver-specific proteins were not substantially decreased as compared with non-insulin-producing cells around the insulin-producing cells. These findings suggest functional hepatocyte-specific characteristics are maintained in insulin-producing cells in the liver. Thus, these hepatocytes were not completely converted to pancreatic cells.

Discussion

In the present study, administration of recombinant adenovirus containing an activated form of PDX1 efficiently induced insulin production in hepatocytes, resulting in reversal of STZ-induced hyperglycemia. The effects were sustained even when exogenous protein expression was no longer detectable. In turn, endogenous PDX1 protein came to be expressed in hepatocytes, which is likely to be the mechanism underlying the sustained effects. On the other hand, albumin and transferrin expressions were observed in insulin-producing cells, suggesting the maintenance of hepatocyte-specific characteristics.

Ferber et al. [7] reported that administration of wt-PDX1 adenovirus at 2×10^9 pfu/mouse ameliorates STZ-induced hyperglycemia but the observed period was very short (no more than 10 days). The same research group also reported the long-term effects of PDX1 gene transfer but the titer of recombinant adenovirus used was relatively high ($1–5 \times 10^{10}$ pfu/mouse) [12]. Such high titers may result in liver damage due to adenoviral toxicity. In the present study, to avoid adenoviral toxicity, recombinant adenoviruses were injected at a titer as low as 2×10^8 pfu. With such a small adenoviral delivery, the wt-PDX1 adenovirus exerted very small effects on insulin and glucose levels, whereas PDX1-VP16 adenovirus substantially increased insulin levels and reversed STZ-induced hyperglycemia. These findings suggest that constitutive activation of PDX1 overcomes the inefficiency associated with low expression levels of PDX1 proteins. Thus, adenoviral transfer of the PDX1-VP16 gene into the liver would presumably be safer than wt-PDX1 gene therapy.

HDAD-mediated PDX1 expression in the liver reportedly causes severe hepatitis including marked inflammatory cell infiltration with focal necrosis associated with expression of pancreatic exocrine genes [10]. In addition, conditional transgenic mice generated by crossing CAG-CAT-PDX1 mice with alb-Cre recombinase-mice also displayed functional liver failure with hepatic expression of exocrine enzymes [11]. In these two models, exogenous PDX1 expression is persistent. Transgenes delivered by HDADs are expressed for long periods exceeding several months. In conditional transgenic mice [11], cells, in which the albumin promoter had once been activated, permanently expressed PDX1 driven by the CAG promoter. These findings suggest that high and persistent expression of PDX1 induces exocrine enzyme expression and thereby liver failure. In the present study, exogenous gene expressions of wt-PDX1 and PDX1-VP16 were transient and expression levels were relatively low on day 7 (Fig. 3A). Thus, transient expression appears to be important for endowing hepatocytes with certain features of pancreatic β cells, but not of exocrine cells.

It is noteworthy that exogenous, transient expression of PDX1-VP16 induced prolonged expression of endogenous PDX1 which apparently contributed to persistent insulin production with hepatocytic features. Ber et al. also reported that rat PDX1 gene transduction using first-generation adenovirus induced persistent endogenous (murine) PDX1 expression. Thus, transient expression of wt-PDX1, and more efficiently PDX1-VP16, may induce persistent and low-level expression of endogenous PDX1. In the adult pancreas, persistent but low-level expression of PDX1 is detected only in β cells [3] and PDX1 expression is required for maintaining normal pancreatic β cell function [6]. These observations suggest that persistent, low-level expression of PDX1 is involved in preferential production of insulin and pancreatic popypeptide in hepatocytes.

In transgenic *Xenopus* tadpoles expressing Xlhbox8 (*Xenopus* homolog of PDX1) carrying the VP16 activation domain under a transthyretin promoter, part or all of the liver is reportedly converted to pancreatic tissue without expression of liver-specific gene products, suggesting complete conversion of hepatocytes to pancreatic cells [14]. In contrast, in the present study, insulin-producing cells in the liver in PDX1-VP16 mice also expressed albumin and transferrin, which suggests preservation of hepatocytic functions. This discrepancy may be explained by the differences between amphibian and mammalian cells. Alternatively, the conversion may occur during embryonic differentiation, while, in adult and differentiated hepatocytes, complete transdifferentiation into pancreatic endocrine or exocrine cells would be difficult to achieve even with PDX1-VP16 expression. Although intensive research is necessary to unravel the precise mechanisms underlying transdifferentiation, the partial conversion induced by PDX1-VP16 expression in adult hepatocytes has practical applications, since loss of hepatocytic functions may result in liver failure. Furthermore, incomplete transdifferentiation could prevent the generated insulin-producing cells from being attacked by a destructive autoimmune response in type 1 diabetics.

Acknowledgments

We thank Dr. H. Kanamori (University of Tokyo) for the generous gift of the VP16 gene. We also thank Ms. I. Sato, K. Kawamura, and M. Hoshi for technical support. This work was supported by a Grant-in-Aid for Scientific Research (B2, 15390282), a Grant-in-Aid for Exploratory Research (15659214) to H. Katagiri, and a Grant-in-Aid for Scientific Research (13204062) to Y. Oka from the Ministry of Education, Science, Sports and Culture of Japan. This work was also supported by Tohoku University 21st Century COE Program "CRESCENDO" to J. Imai, J. Gao, and H. Katagiri.

References

[1] A.M. Shapiro, J.R. Lakey, E.A. Ryan, G.S. Korbutt, E. Toth, G.L. Warnock, N.M. Kneteman, R.V. Rajotte, Islet transplantation in seven patients with type 1 diabetes mellitus using a glucocorticoid-free immunosuppressive regimen, N. Engl. J. Med. 343 (2000) 230–238.

[2] G. Deutsch, J. Jung, M. Zheng, J. Lora, K.S. Zaret, A bipotential precursor population for pancreas and liver within the embryonic endoderm, Development 128 (2001) 871–881.

[3] H. Ohlsson, K. Karlsson, T. Edlund, Ipf1, a homeodomain-containing transactivator of the insulin gene, EMBO J. 12 (1993) 4251–4259.

[4] M.F. Offield, T.L. Jetton, P.A. Labosky, M. Ray, R.W. Stein, M.A. Magnuson, B.L. Hogan, C.V. Wright, Pdx-1 is required for pancreatic outgrowth and differentiation of the rostral duodenum, Development 122 (1996) 983–995.

[5] J. Jonsson, L. Carlsson, T. Edlund, H. Edlund, Insulin-promoter-factor 1 is required for pancreas development in mice, Nature 371 (1994) 606–609.

[6] U. Ahlgren, J. Jonsson, L. Jonsson, K. Simu, H. Edlund, Beta-cell-specific inactivation of the mouse ipf1/pdx1 gene results in loss of the beta-cell phenotype and maturity onset diabetes, Genes Dev. 12 (1998) 1763–1768.

[7] S. Ferber, A. Halkin, H. Cohen, I. Ber, Y. Einav, I. Goldberg, I. Barshack, R. Seijffers, J. Kopolovic, N. Kaiser, A. Karasik, Pancreatic and duodenal homeobox gene 1 induces expression of insulin genes in liver and ameliorates streptozotocin-induced hyperglycemia, Nat. Med. 6 (2000) 568–572.

[8] A. Grapin-Botton, A.R. Majithia, D.A. Melton, Key events of pancreas formation are triggered in gut endoderm by ectopic expression of pancreatic regulatory genes, Genes Dev. 15 (2001) 444–454.

[9] R.S. Heller, D.A. Stoffers, M.A. Hussain, C.P. Miller, J.F. Habener, Misexpression of the pancreatic homeodomain protein idx-1 by the hoxa-4 promoter associated with agenesis of the cecum, Gastroenterology 115 (1998) 381–387.

[10] H. Kojima, M. Fujimiya, K. Matsumura, P. Younan, H. Imaeda, M. Maeda, L. Chan, Neurod-betacellulin gene therapy induces islet neogenesis in the liver and reverses diabetes in mice, Nat. Med. 9 (2003) 596–603.
[11] T. Miyatsuka, H. Kaneto, Y. Kajimoto, S. Hirota, Y. Arakawa, Y. Fujitani, Y. Umayahara, H. Watada, Y. Yamasaki, M.A. Magnuson, J. Miyazaki, M. Hori, Ectopically expressed pdx-1 in liver initiates endocrine and exocrine pancreas differentiation but causes dysmorphogenesis, Biochem. Biophys. Res. Commun. 310 (2003) 1017–1025.
[12] I. Ber, K. Shternhall, S. Perl, Z. Ohanuna, I. Goldberg, I. Barshack, L. Benvenisti-Zarum, I. Meivar-Levy, S. Ferber, Functional, persistent, and extended liver to pancreas transdifferentiation, J. Biol. Chem. 278 (2003) 31950–31957.
[13] S. Dutta, M. Gannon, B. Peers, C. Wright, S. Bonner-Weir, M. Montminy, Pdx:Pbx complexes are required for normal proliferation of pancreatic cells during development, Proc. Natl. Acad. Sci. USA 98 (2001) 1065–1070.
[14] M.E. Horb, C.N. Shen, D. Tosh, J.M. Slack, Experimental conversion of liver to pancreas, Curr. Biol. 13 (2003) 105–115.
[15] H. Mizuguchi, M.A. Kay, Efficient construction of a recombinant adenovirus vector by an improved in vitro ligation method, Hum. Gene Ther. 9 (1998) 2577–2583.
[16] H. Mizuguchi, M.A. Kay, A simple method for constructing e1- and e1/e4-deleted recombinant adenoviral vectors, Hum. Gene Ther. 10 (1999) 2013–2017.
[17] T. Anno, S. Uehara, H. Katagiri, Y. Ohta, K. Ueda, H. Mizuguchi, Y. Moriyama, Y. Oka, Y. Tanizawa, Overexpression of constitutively activated glutamate dehydrogenase induces insulin secretion through enhanced glutamate oxidation, Am. J. Physiol. Endocrinol. Metab. 286 (2004) E280–E285.
[18] H. Katagiri, T. Asano, H. Ishihara, K. Inukai, Y. Shibasaki, M. Kikuchi, Y. Yazaki, Y. Oka, Overexpression of catalytic subunit p110alpha of phosphatidylinositol 3-kinase increases glucose transport activity with translocation of glucose transporters in 3t3-l1 adipocytes, J. Biol. Chem. 271 (1996) 16987–16990.
[19] I. Sadowski, J. Ma, S. Triezenberg, M. Ptashne, Gal4-vp16 is an unusually potent transcriptional activator, Nature 335 (1988) 563–564.
[20] S.J. Triezenberg, R.C. Kingsbury, S.L. McKnight, Functional dissection of vp16, the trans-activator of herpes simplex virus immediate early gene expression, Genes Dev. 2 (1988) 718–729.
[21] Y. Ishigaki, S. Oikawa, T. Suzuki, S. Usui, K. Magoori, D.H. Kim, H. Suzuki, J. Sasaki, H. Sasano, M. Okazaki, T. Toyota, T. Saito, T.T. Yamamoto, Virus-mediated transduction of apolipoprotein e (apoe)-sendai develops lipoprotein glomerulopathy in apoe-deficient mice, J. Biol. Chem. 275 (2000) 31269–31273.
[22] M.J. Peeters, G.A. Patijn, A. Lieber, L. Meuse, M.A. Kay, Adenovirus-mediated hepatic gene transfer in mice: comparison of intravascular and biliary administration, Hum. Gene Ther. 7 (1996) 1693–1699.

J Hum Genet (2005) 50:92–98
DOI 10.1007/s10038-004-0225-5

ORIGINAL ARTICLE

Naoko Iwasaki · Yukio Horikawa · Takafumi Tsuchiya
Yutaka Kitamura · Takahiro Nakamura
Yukio Tanizawa · Yoshitomo Oka · Kazuo Hara
Takashi Kadowaki · Takuya Awata · Masashi Honda
Katsuko Yamashita · Naohisa Oda · Li Yu
Norihiro Yamada · Makiko Ogata · Naoyuki Kamatani
Yasuhiko Iwamoto · Laura del Bosque-Plata
M. Geoffrey Hayes · Nancy J. Cox · Graeme I. Bell

Genetic variants in the calpain-10 gene and the development of type 2 diabetes in the Japanese population

Received: 14 September 2004 / Accepted: 10 December 2004 / Published online: 5 February 2005

Abstract Variation in the gene encoding the cysteine protease calpain-10 has been linked and associated with risk of type 2 diabetes. We have examined the effect of three polymorphisms in the calpain-10 gene (SNP-43, Indel-19, and SNP-63) on the development of type 2 diabetes in the Japanese population in a pooled analysis of 927 patients and 929 controls. We observed that SNP-43, Indel-19, and SNP-63 either individually or as a haplotype were not associated with altered risk of type 2 diabetes with the exception of the rare 111/221 haplogenotype (odds ratio (OR) = 3.53, $P = 0.02$). However, stratification based on the median age-at-diagnosis in the pooled study population (< 50 and ≥50 years) revealed that allele 2 of Indel-19 and the 121 haplotype were associated with reduced risk in patients with later age-at-diagnosis (age-at-diagnosis ≥50 years OR = 0.82 and 0.80, respectively; $P = 0.04$ and 0.02). Thus, variation in the calpain-10 gene may affect risk of type 2 diabetes in Japanese, especially in older individuals.

Keywords Association study · Age-at-diagnosis · Calpain-10 · Genetics · Polymorphism · Type 2 diabetes

Naoko Iwasaki, Yukio Horikawa and Takafumi Tsuchiya contributed equally to this work.

N. Iwasaki (✉) · M. Ogata · Y. Iwamoto
Diabetes Center, Tokyo Women's Medical University,
8-1 Kawada-cho, Shinjuku-ku,
Tokyo 162-8666, Japan
E-mail: niwasaki@dmc.twmu.ac.jp
Tel.: +81-3-33538111
Fax: +81-3-33581941

Y. Horikawa · L. Yu · N. Yamada
Laboratory of Molecular Genetics,
Department of Cell Biology,
Institute for Molecular and Cellular Regulation,
Gunma University, Maebashi, Japan

T. Tsuchiya · L. del Bosque-Plata · M. G. Hayes · N. J. Cox · G. I. Bell
Departments of Biochemistry and Molecular Biology,
Human Genetics and Medicine,
The University of Chicago,
Chicago, Illinois, USA

Y. Kitamura · T. Nakamura · N. Kamatani
Department of Statistical Genetics,
Institute of Rheumatology,
Tokyo Women's Medical University,
Tokyo, Japan

Y. Tanizawa
Division of Molecular Analysis of Human Disorders,
Department of Bio-Signal Analysis,
Yamaguchi University Graduate School of Medicine,
Ube, Japan

Y. Oka
Division of Molecular Metabolism and Diabetes,
Department of Internal Medicine,
Tohoku University, Sendai, Japan

K. Hara · T. Kadowaki
Department of Metabolic diseases,
Graduate School of Medicine and Faculty of Medicine,
University of Tokyo, Tokyo, Japan

T. Awata
Division of Endocrinology and Diabetes, Department of Medicine,
Saitama Medical School, Saitama, Japan

M. Honda
Shiseikai Daini Hospital, Tokyo, Japan

K. Yamashita
Seijin Igaku Medical Clinic, Tokyo, Japan

N. Oda
Department of Internal Medicine,
Fujita Health University School of Medicine,
Aichi, Japan

Introduction

The results of association and linkage studies indicate that multiple genes are involved in determining susceptibility to type 2 diabetes in Japanese with each gene making a modest contribution to overall risk (Seino et al. 2001; Mori et al. 2001, 2002; Iwasaki et al. 2003). The gene encoding the cysteine protease calpain-10 (CAPN10) was first found to be associated with risk of type 2 diabetes in studies carried out in Mexican Americans (Horikawa et al. 2000). Two recent meta-analyses and a large association study have confirmed that single nucleotide polymorphisms (SNP)-43 and SNP-44 are associated with a 1.19- and 1.17-fold increased risk, respectively, of type 2 diabetes (Weedon et al. 2003; Song et al. 2004). SNP-43 may be a functional polymorphism affecting transcriptional regulation of the calpain-10 gene (Horikawa et al. 2000; Baier et al. 2000). However, Indel-19 and SNP-63 are just tagging SNPs, and their effect on transcriptional regulation or other functions of calpain-10 are unknown. The effect of the core CAPN10 polymorphisms SNP-43, Indel-19, and SNP-63 on risk of type 2 diabetes in Japanese has been examined in three small studies (Daimon et al. 2002; Horikawa et al. 2003; Shima et al. 2003). The results suggest that variation in CAPN10 is not a major risk factor. However, these studies were not able to quantify the effect of CAPN10 on risk because of the small number of cases and controls in the individual studies. Here, we reexamine the role of the CAPN10 in the development of type 2 diabetes in the Japanese population.

Material and methods

Subjects

All subjects were Japanese. We studied three groups of cases and controls. The first group (study 1) included 205 unrelated subjects with type 2 diabetes recruited from the outpatient clinic in the Diabetes Center, Tokyo Women's Medical University and 208 unrelated normoglycemic subjects recruited from the Seijin Igaku Medical Clinic of Tokyo Women's Medical University using the following inclusion criteria: age >60 years, HbA1c $<5.6\%$, and no family history of diabetes. The second group (study 2) consisted of 281 unrelated normal glucose-tolerant (by oral glucose tolerance testing) subjects who were recruited at four outpatient clinics: Diabetes Center, Tokyo Women's Medical University ($n=50$); Third Department of Internal Medicine, Yamaguchi University ($n=121$); Department of Internal Medicine, University of Tokyo ($n=30$); and Shiseikai Daini Hospital, Tokyo ($n=80$). The third group of subjects (study 3) comprised 454 patients with type 2 diabetes and 192 nondiabetic controls who were recruited from Gunma University Hospital and affiliated hospitals and Fujita Health University School of Medicine. The genetic studies were approved by the institutional review board of each participating institution. Informed consent was obtained from all participants.

The pooled analyses included the datasets above as well as the data from three published studies: Daimon et al. 2002, SNP-43; Horikawa et al. 2003, SNP-43, Indel-19 and SNP-63; and Shima et al. 2003, SNP-43, Indel-19, and SNP-63.

Linkage disequilibrium (LD)

We examined the structure of the linkage disequilibrium (LD) in the CAPN10 region using the software package GOLD [graphical overview of linkage disequilibrium (Abecasis and Cookson 2000)] and a common set of 14 SNPs having a minor allele frequency ≥ 0.10 in diabetic ($n=30$) and nondiabetic subjects ($n=30$).

Genotyping

Genomic DNA was prepared from peripheral blood lymphocytes by standard procedures. We typed three polymorphisms in CAPN10: SNP-43, CAPN10-g.4852G>A (rs3792267); insertion/deletion (Indel)-19, CAPN10-g.7920 (32 bp-repeats) (rs3842570); and CAPN10-g.16378C>T (rs5030952) as described previously (Horikawa et al. 2003) or using TaqMan-based assays with custom probes/primers (Applied Biosystems, Foster City, CA, USA). Additional SNPs used for studies of LD in the CAPN10 region were genotyped using TaqMan technology. Previous studies have shown that the three core polymorphisms lead to four common haplotypes described as 111, 112, 121, and 221 (allele 1 or 2 at SNP-43, Indel-19, and SNP-63, respectively). The haplogenotypes were assigned by inspection of the genotypes at SNP-43, Indel-19, and SNP-63.

Statistical analyses

Polymorphisms were tested for deviation from Hardy-Weinberg equilibrium, heterogeneity in allele and genotype among studies and differences in allele, genotype, haplotype, and haplogenotype between groups using a chi-squared test. All P values are two sided.

Results

Haplotype structure across the CAPN10 region

The analysis of LD in the region of CAPN10 revealed a single region of strong LD (Fig. 1).

CAPN10 and SNP-43, and Indel-19 and SNP-63 are contained within this single LD block, which does not

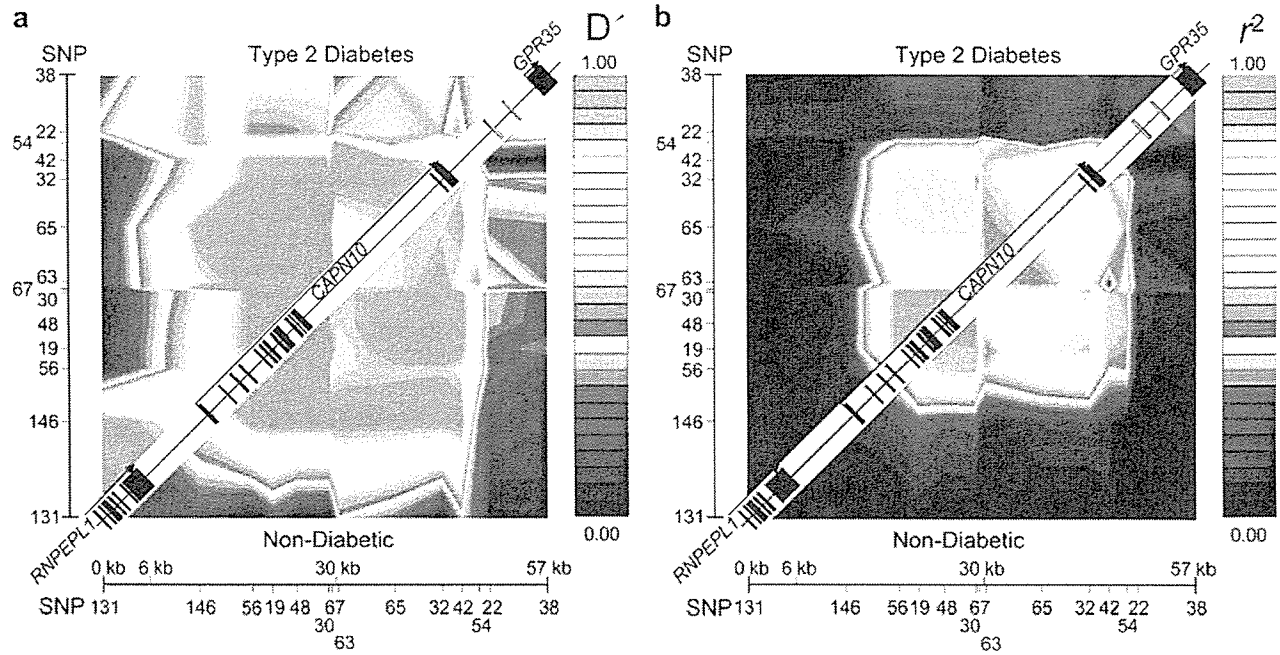

Fig. 1 Linkage disequilibrium (LD) in the CAPN10 region visualized using GOLD. The red and orange regions denote strong LD as defined using D' and r^2. The exons of CAPN10 and the adjacent genes RNPEPL1 and GPR35 are shown as *filled boxes* along the diagonal. The two variable number of tandem repeats (*VNTRs*) between CAPN10 and GPR35 are shown as *open boxes*. The SNPs used in this analysis are described in Horikawa et al. (2000). SNP-43 was not included in this analysis because the minor allele frequency was <0.10 in the Japanese population

include the flanking RNPEPL1 and GPR35 genes. Thus, association of polymorphisms in this block with type 2 diabetes or a type-2-diabetes-related trait in the Japanese population implies that it is a variation in CAPN10 itself and not an adjacent locus that is responsible for the effect. The associated variant may or may not be causal depending on the LD with other variants in the block.

Genetic variation in CAPN10 and type 2 diabetes

We typed SNP-43, Indel-19, and SNP-63 in the three study groups described above (Table 1). There was no significant difference in the frequency of SNP-43 or Indel-19 between cases and controls (Table 2), which is in agreement with previous studies in Japanese (Daimon et al. 2002; Horikawa et al. 2003). However, we observed a significant difference in SNP-63 allele frequency between cases and controls in the subjects from study 1 (0.66 and 0.73, respectively, $P=0.04$) but not in the subjects from study 3 (Table 2). In order to gain a better understanding of what role SNP-63 may play in the progression of type 2 diabetes, we examined the effect of SNP-63 genotype on various clinical and metabolic characteristics assessed by a standard 75-g oral glucose tolerance test in a group of 281 normal glucose-tolerant subjects from study 2 (Table 3). No significant effects of SNP-63 genotype on phenotype were observed except for area-under-the-curve plasma glucose level from 0 min to 120 min ($P=0.03$).

We then carried out a pooled analysis using data from all known studies carried out in the Japanese population (Daimon et al. 2002; Horikawa et al. 2003; Shima et al. 2003). The 281 nondiabetic subjects from study 2 were excluded from the primary analyses because their mean age-at-study in this group was significantly younger than other the control groups. The pooled study population included 927 patients and 929 controls although Indel-19 and SNP-63 were not typed in all subjects. There was no significant difference in SNP-43, Indel-19, or SNP-63 genotype or allele frequencies between the type 2 diabetic and control groups in the overall analysis (Table 4). There was also no significant difference in SNP-43/Indel-19/SNP-63 haplotype (Table 5) or haplogenotype frequency (Table 6) except for the rare 111/221 combination, which was associated with significantly increased risk of type 2 diabetes (OR = 3.53, $P=0.02$).

Genetic variation in CAPN10 may modify risk of type 2 diabetes in older patients

Since age is a risk factor for type 2 diabetes, we split the type 2 diabetic group based on median age-at-diagnosis, which was 50 years in the pooled sample, and repeated the comparisons but using only those cases for whom age-at-diagnosis was available: Patients with age-at-diagnosis <50 years included 118 patients from study 1, 103 from study 3, and 68 from Horikawa et al. (2003); and patients with age-at-diag-

Table 1 Clinical characteristics of study populations. Data are mean ± SD. *NA* data not available, *Ctrl* control, *T2D* type 2 diabetes

Trait	Study population											
	Study 1		Study 2		Study 3		Horikawa et al. (2003)		Shima et al. (2003)		Daimon et al. (2002)	
Subjects	Ctrl[a]	T2D	Ctrl	T2D	Ctrl[a]	T2D	Ctrl[a]	T2D	Ctrl	T2D	Ctrl	T2D
n	208	205	281	–	192	454	172	177	276	10	81	81
Gender (F/M)	68/140	84/121	135/146	–	70/122	206/248	90/82	63/114	NA	NA	46/35	45/36
Age-at-study (years)	67.9 ± 5.5	59.1 ± 13.0	44.4 ± 15.9	–	67.8 ± 5.6	59.9 ± 11.7	68.0 ± 5.7	62.0 ± 11.0	NA	NA	62.3 ± 8.2	65.1 ± 10.7
Age-at-diagnosis (years)	–	45.9 ± 12.7	–	–	–	51.0 ± 12.0[b]	–	49.8 ± 11.4	–	NA	–	NA
BMI	23.1 ± 2.4	23.5 ± 3.6	22.3 ± 3.0	–	23.1 ± 2.8	24.2 ± 4.2	22.8 ± 3.3	23.9 ± 3.3	NA	NA	23.8 ± 3.6	25.6 ± 3.9
HbA_{1c} (%)	5.0 ± 0.3	8.2 ± 2.0	4.9 ± 0.4	–	4.9 ± 0.3	7.9 ± 1.9	5.0 ± 0.4	6.7 ± 1.0	NA	NA	5.3 ± 0.3	6.7 ± 1.1
Fasting glucose (mg/dl)	95.0 ± 8.7	160.5 ± 48.5	92.8 ± 9.4	–	NA	NA	NA	NA	NA	NA	NA	NA
Treatment (diet/oral agents/insulin)	–	42/81/82	–	–	–	NA	–	46/70/61	–	NA	–	NA

[a] All subjects were > 60 years old
[b] Data are available for only 246 subjects

nosis ≥50 years included 87 patients from study 1, 143 from study 3, and 85 from Horikawa et al. (2003). There was no significant difference in SNP-43, Indel-19, and SNP-63 allele or genotype frequencies between the type 2 diabetic group with age-at-diagnosis < 50 years and the controls (Table 4). The SNP-43 and SNP-63 frequencies were also not different between the type 2 diabetic group with age-at-diagnosis ≥50 years and the controls. However, there was a small but significant difference in Indel-19 allele frequency (Table 4). The 3R allele at Indel-19 (allele 2 in the haplotype) was associated with lower risk of type 2 diabetes (OR = 0.82, $P = 0.04$).

The 121 haplotype was associated with significantly decreased risk (OR = 0.80, $P = 0.02$) of type 2 diabetes in the group of patients with age-at-diagnosis ≥50 years (Table 5). The 111 haplotype had the highest risk (OR = 1.33, $P = 0.046$) in the older group of patients. This effect of the 111 haplotype likely reflects the contribution of SNP-44 to type 2 diabetes risk (Weedon et al. 2003) since 88% of the 111 haplotypes in Japanese carry the at-risk C-allele at SNP-44. The rare 111/221 haplogenotype was associated with increased risk of type 2 diabetes irrespective of age-at-diagnosis (Table 6). The 121/121 haplogenotype had a protective effect against type 2 diabetes that approached significance in patients with age-at-diagnosis ≥50 years (OR = 0.76, $P = 0.06$). Individuals with haplotypes 111/111, 111/112, and 111/221 had the highest risk of type 2 diabetes (OR = 1.83, 1.25, and 4.12, respectively) although the increase in risk was not significant because of the small numbers of individuals studied. If the nondiabetic subjects in study 2 (Table 1) are included in the pooled control group, the results are similar, including the effects of the 121/121 haplogenotype on risk in patients with age-at-diagnosis ≥50 years (OR = 0.75, $P = 0.04$).

Discussion

The results suggest that genetic variation in CAPN10 may affect risk of type 2 diabetes in the Japanese population, especially in older individuals. Interestingly, the common 121 haplotype appears to be protective in Japanese, suggesting the overall effect of CAPN10 in this population is to reduce the risk of diabetes rather than increase it. It is important to note, though, that the statistical significance of the comparison is marginal ($P = 0.01$–0.04), and none of the comparisons would be significant if corrected for multiple testing. Thus, the results presented here need to be confirmed through studies of a much larger dataset. However, if our results are correct, they suggest an interaction between genetic (CAPN10) and nongenetic (age) factors to modify risk of type 2 diabetes. In this regard, recent studies have shown that calpain-10 is part of a novel apoptotic pathway in insulin-secreting pancreatic beta cells and thus may

Table 2 Genotype and allele frequencies of CAPN10 polymorphisms in Japanese. The number of subjects of each genotype are indicated. All genotypic distributions are in Hardy-Weinberg equilibrium. *NA* not available, *Ctrl* control, *T2D* type 2 diabetes

Marker	Subjects	Genotype	This study 1	This study 2	This study 3	Horikawa et al. (2003)	Shima et al. (2003)	Daimon et al. (2002)	*P* for heterogeneity
SNP-43	Ctrl	G/G	188	251	165	154	252	76	
		G/A	20	29	24	18	24	5	
		A/A	0	1	0	0	0	0	0.75
		Allele frequency	G: 0.95	G: 0.94	G: 0.94	G: 0.95	G: 0.96	G: 0.97	
			A: 0.05	A: 0.06	A: 0.06	A: 0.05	A: 0.04	A: 0.03	0.62
	T2D	G/G	184	NA	389	158	8	76	
		G/A	21	NA	57	19	2	5	
		A/A	0	NA	1	0	0	0	0.75
		Allele frequency	G: 0.95	NA	G: 0.93	G: 0.95	G: 0.90	G: 0.97	
			A: 0.05		A: 0.07	A: 0.05	A: 0.10	A: 0.03	0.37
Indel-19[a]	Ctrl	2R/2R	27	42	35	23	42	NA	
		2R/3R	99	126	78	78	126	NA	
		3R/3R	82	113	73	71	108	NA	0.90
		Allele frequency	2R: 0.37	2R: 0.37	2R: 0.40	2R: 0.36	2R: 0.38	NA	
			3R: 0.63	3R: 0.63	3R: 0.60	3R: 0.64	3R: 0.62		0.86
	T2D	2R/2R	32	NA	63	28	1	NA	
		2R/3R	104	NA	209	82	3	NA	
		3R/3R	69	NA	176	67	6	NA	0.62
		Allele frequency	2R: 0.41	NA	2R: 0.37	2R: 0.39	2R: 0.25	NA	
			3R: 0.59		3R: 0.63	3R: 0.61	3R: 0.75		0.34
SNP-63	Ctrl	C/C	111	151	99	90	151	NA	
		C/T	81	106	65	70	103	NA	
		T/T	16	24	18	12	22	NA	0.99
		Allele frequency	C: 0.73	C: 0.73	C: 0.72	C: 0.73	C: 0.73	NA	
			T: 0.27	T: 0.27	T: 0.28	T: 0.27	T: 0.27		0.99
	T2D	C/C	90	NA	255	93	6	NA	
		C/T	92	NA	165	74	3	NA	
		T/T	23	NA	30	10	1	NA	0.09
		Allele frequency	C: 0.66	NA	C: 0.75	C: 0.73	C: 0.75	NA	
			T: 0.34		T: 0.25	T: 0.27	T: 0.25		0.03

[a] Indel-19 is a diallelic insertion/deletion polymorphism with alleles of two repeats (2R) or three repeats (3R) of a 32-bp sequence

Table 3 Clinical and metabolic characteristics of normal glucose tolerant subjects (study 2) by SNP-63 genotype. Data are mean ± SD. Subjects underwent a standard 75-g oral glucose tolerance test with glucose and insulin determined at 0′, 30′, 60′, and 120′. The number of individuals in each group for determination of insulinogenic index and HOMA are noted in parentheses. *BMI* body mass index, *AUC* area under the curve

Trait	Genotype			*P*[a]
	C/C	C/T	T/T	
n	150	105	25	
Gender (M/F)	72/78	59/46	14/11	0.40
Age (years)	45.0 ± 14.9	43.8 ± 16.7	44.4 ± 18.7	0.72
BMI (kg/m2)	22.3 ± 2.5	22.2 ± 3.6	22.6 ± 3.0	0.70
HbA1c (%)	4.9 ± 0.4	4.9 ± 0.4	5.0 ± 0.4	0.79
Plasma glucose (mg/dl)				
0 min	93.1 ± 9.6	92.2 ± 9.1	94.1 ± 8.8	0.51
120 min	104.1 ± 18.5	106.1 ± 18.8	108.2 ± 14.5	0.30
AUC 0-120′	14,510.6 ± 2706.2	15,233.4 ± 2937.1	15,043.2 ± 3056.1	0.03
Plasma insulin (μU/ml)				
0 min	6.4 ± 2.2	6.4 ± 2.6	6.5 ± 4.4	0.81
120 min	30.6 ± 16.9	32.0 ± 16.8	30.1 ± 20.2	0.74
AUC 0-120′	3,972.4 ± 2030.8	4,267.4 ± 1816.9	4,049.2 ± 1969.1	0.44
Insulinogenic index	0.89 ± 0.89 (147)	0.96 ± 3.62 (101)	1.14 ± 1.85 (24)	0.08
HOMA	1.43 ± 0.53 (146)	1.41 ± 0.54 (101)	1.30 ± 0.63 (23)	0.35

[a] *P* value by ANCOVA with institution, gender, and genotype as independent factors and age and BMI as covariates

affect the response of the beta cell to aging or its ability to compensate in response to an increasing demand for insulin (Johnson et al. 2004).

The observation that individuals homozygous for the 121 haplotype may be at increased risk of type 2 diabetes in some European populations (Orho-

Table 4 SNP-43, Indel-19, and SNP-63 and type 2 diabetes in Japanese—a pooled analysis. The number of subjects of each genotype are indicated. All genotypic distributions are in Hardy-Weinberg equilibrium. The cases were divided into two groups based on the median age-at-diagnosis in the pooled sample—50 years. Note that age-at-diagnosis was not available for all subjects

Marker	Genotype	Overall			Age-at-diagnosis < 50 years		Age-at-diagnosis ≥50 years	
		Ctrl	T2D	*P*	T2D	*P*	T2D	*P*
SNP-43	G/G	833	811		255		276	
	G/A	91	104		28	0.98	32	0.78
	A/A	0	1	0.35	0		0	
	Allele frequency	G: 0.95	G: 0.94		G: 0.95		G: 0.95	
		A: 0.05	A: 0.06	0.25	A: 0.05	0.98	A: 0.05	0.79
Indel-19[a]	2R/2R	127	124		36		58	
	2R/3R	381	396		143		151	0.11
	3R/3R	334	316	0.67	107	0.33	105	
	Allele frequency	2R: 0.38	2R: 0.39		2R: 0.38		2R: 0.43	
		3R: 0.62	3R: 0.61	0.69	3R: 0.62	0.91	3R: 0.57	0.04
SNP-63	C/C	451	443		149		151	
	C/T	319	333		125		129	
	T/T	68	62	0.72	14	0.09	28	0.35
	Allele frequency	C: 0.73	C: 0.73		C: 0.73		C: 0.71	
		T: 0.27	T: 0.27	0.94	T: 0.27	0.79	T: 0.29	0.17

[a] Indel-19: 2R, 2 repeats of 32-bp sequence; 3R, 3 repeats

Table 5 CAPN10 haplotype frequency and risk of type 2 diabetes in Japanese—a pooled analysis. The haplotypes are those defined by SNP-43, Indel-19, and SNP-63, and the specific alleles are: SNP-43, allele 1, G and allele 2, A; Indel-19, allele 1, 2 repeats of 32-bp sequence, and allele 2, 3 repeats; and SNP-63, allele 1, C, and allele 2, T. The cases were divided into two groups based on the median age-at-diagnosis in the pooled sample—50 years. Note that age-at-diagnosis was not available for all subjects. *Ctrl* control, *T2D* type 2 diabetes

Haplotype	Overall				Age-at-diagnosis < 50 years			Age-at-diagnosis ≥50 years		
	Ctrl (n=825)	T2D (n=827)	OR (95% CI)[a]	*P*	T2D (n=277)	OR (95% CI)[a]	*P*	T2D (n=305)	OR (95% CI)[a]	*P*
111	0.106	0.113	1.07 (0.86–1.34)	0.52	0.117	1.12 (0.83–1.52)	0.46	0.136	1.33 (1.00–1.75)	0.05
121	0.572	0.553	0.93 (0.81–1.07)	0.29	0.567	0.98 (0.81–1.19)	0.85	0.515	0.80 (0.66–0.96)	0.02
112	0.270	0.274	1.02 (0.88–1.19)	0.79	0.265	0.98 (0.78–1.21)	0.82	0.297	1.14 (0.93–1.40)	0.21
221	0.052	0.059	1.15 (0.85–1.54)	0.37	0.051	0.97 (0.62–1.50)	0.88	0.052	1.01 (0.66–1.53)	0.97

[a] The OR and 95% CI of each haplotype relative to other haplotypes as a group are shown

Table 6 CAPN10 haplogenotype and risk of type 2 diabetes in Japanese—a pooled analysis. The haplotypes are those defined by SNP-43, Indel-19, and SNP-63, and the specific alleles are indicated in the legend to Table 5. The number of individuals with each haplogenotype is indicated

Haplogenotype	Overall				Age-at-diagnosis < 50 years			Age-at-diagnosis ≥ 50 years		
	Ctrl	T2D	OR (95% CI)[a]	*P*	T2D	OR (95% CI)[a]	*P*	T2D	OR (95% CI)[a]	*P*
111/111	15	18	1.20 (0.60–2.40)	0.60	5	0.99 (0.36–2.76)	0.99	10	1.83 (0.82–4.07)	0.14
111/121	97	93	0.95 (0.70–1.29)	0.74	31	0.95 (0.62–1.45)	0.80	37	1.04 (0.69–1.55)	0.86
111/112	44	44	1.00 (0.65–1.53)	0.99	18	1.23 (0.70–2.17)	0.47	20	1.25 (0.72–2.15)	0.43
111/221	4	14	3.53 (1.24–10.1)	0.02	6	4.54 (1.42–14.5)	0.01	6	4.12 (1.27–13.3)	0.02
112/112	66	62	0.93 (0.65–1.34)	0.70	13	0.57 (0.31–1.04)	0.06	27	1.12 (0.70–1.78)	0.64
112/121	247	254	1.04 (0.84–1.28)	0.73	90	1.13 (0.84–1.51)	0.43	97	1.09 (0.82–1.45)	0.55
112/221	23	32	1.40 (0.82–2.41)	0.22	13	1.72 (0.86–3.41)	0.12	10	1.18 (0.56–2.51)	0.66
121/121	270	259	0.94 (0.76–1.15)	0.54	92	1.02 (0.77–1.37)	0.88	82	0.76 (0.56–1.01)	0.06
121/221	59	50	0.84 (0.57–1.23)	0.37	9	0.44 (0.22–0.87)	0.02	16	0.72 (0.41–1.27)	0.25
221/221	0	1	–	–	0			0		

[a] The OR and 95% CI of each haplogenotype relative to the other haplotype combinations as a group are shown

Melander et al. 2002; Malecki et al. 2002) but at decreased risk in older Japanese raises the possibility that additional genetic variation may distinguish high- and low-risk subtypes of the 121 haplotype. Transpopulation mapping may be a useful strategy for identifying this variation.

Acknowledgements The authors thank Ms. A. Nogami, Ms. M. Y. Sagisaka, and Mr. M. Ikeda for their skillful technical assistance. This study was supported by Grants-in-Aid for Scientific Research C (10671084, 10470234) and for Scientific Research on Priority Areas Medical Genome Science from the Japan Ministry of Science, Education, Sports, Culture and Technology (12204102, 13204082, 14013059, 15012250), Novo Nordisk Foundation, the Naito Foundation (to N.I.) and Grants-in-Aid for Scientific Research B (13470223, 13557091) (to Y.H.), and U.S. Public Health Service (Grants DK-20595, −47486 and −55889). G.I.B. is an Investigator of the Howard Hughes Medical Institute.

References

Abecasis GR, Cookson WO (2000) GOLD–graphical overview of linkage disequilibrium. Bioinformatics 16:182–183

Baier LJ, Permana PA, Yang X, Pratley RE, Hanson RL, Shen GQ, Mott D, Knowler WC, Cox NJ, Horikawa Y, Oda N, Bell GI, Bogardus C (2000) A 1-10 gene polymorphism is associated with reduced muscle mRNA levels and insulin resistance. J Clin Invest 106:R69-R73

Daimon M, Oizumi T, Saitoh T, Kameda W, Yamaguchi H, Ohnuma H, Igarashi M, Manaka H, Kato T (2002) Calpain-10 gene polymorphisms are related, not to type 2 diabetes, but to increased serum cholesterol in Japanese. Diabetes Res Clin Pract 56:147–152

Horikawa Y, Oda N, Cox NJ, Li X, Orho-Melander M, Hara M, Hinokio Y, Lindner TH, Mashima H, Schwarz PE, del Bosque-Plata L, Oda Y, Yoshiuchi I, Colilla S, Polonsky KS, Wei S, Concannon P, Iwasaki N, Schulze J, Baier LJ, Bogardus C, Groop L, Boerwinkle E, Hanis CL, Bell GI (2000) Genetic variation in the gene encoding calpain-10 is associated with type 2 diabetes mellitus. Nat Genet 26:163–175

Horikawa Y, Oda N, Yu L, Imamura S, Fujiwara K, Makino M, Seino Y, Itoh M, Takeda J (2003) Genetic variations in calpain-10 gene are not a major factor in the occurrence of type 2 diabetes in Japanese. J Clin Endocrinol Metab 88:244–247

Iwasaki N, Cox NJ, Wang YQ, Schwarz PE, Bell GI, Honda M, Imura M, Ogata M, Saito M, Kamatani N, Iwamoto Y (2003) Mapping genes influencing type 2 diabetes risk and BMI in Japanese subjects. Diabetes 52:209–213

Johnson JD, Han Z, Otani K, Ye H, Zhang H, Wu H, Horikawa Y, Misler S, Bell GI, Polonsky KS (2004) RyR2 and calpain-10 delineate a novel apoptosis pathway in pancreatic islets. J Biol Chem 279:24794–24802

Malecki MT, Moczulski DK, Klupa T, Wanic K, Cyganek K, Frey J, Sieradzki J (2002) Homozygous combination of calpain 10 gene haplotypes is associated with type 2 diabetes mellitus in a Polish population. Eur J Endocrinol 146:695–699

Mori H, Ikegami H, Kawaguchi Y, Seino S, Yokoi N, Takeda J, Inoue I, Seino Y, Yasuda K, Hanafusa T, Yamagata K, Awata T, Kadowaki T, Hara K, Yamada N, Gotoda T, Iwasaki N, Iwamoto Y, Sanke T, Nanjo K, Oka Y, Matsutani A, Maeda E, Kasuga M (2001) The Pro12 → Ala substitution in PPAR-γ is associated with resistance to development of diabetes in the general population: possible involvement in impairment of insulin secretion in individuals with type 2 diabetes. Diabetes 50:891–894

Mori Y, Otabe S, Dina C, Yasuda K, Populaire C, Lecoeur C, Vatin V, Durand E, Hara K, Okada T, Tobe K, Boutin P, Kadowaki T, Froguel P (2002) Genome-wide search for type 2 diabetes in Japanese affected sib-pairs confirms susceptibility genes on 3q, 15q, and 20q and identifies two new candidate Loci on 7p and 11p. Diabetes 51:1247–1255

Orho-Melander M, Klannemark M, Svensson MK, Ridderstrale M, Lindgren CM, Groop L (2002) Variants in the calpain-10 gene predispose to insulin resistance and elevated free fatty acid levels. Diabetes 51:2658–2664

Seino S on behalf of the Study Group of Comprehensive Analysis of Genetic Factors in Diabetes Mellitus (2001) S20G mutation of the amylin gene is associated with Type II diabetes in Japanese. Diabetologia 44:906–909

Shima Y, Nakanishi K, Odawara M, Kobayashi T, Ohta H (2003) Association of the SNP-19 genotype 22 in the calpain-10 gene with elevated body mass index and hemoglobin A1c levels in Japanese. Clin Chim Acta 336:89–96

Song Y, Niu T, Manson JE, Kwiatkowski DJ, Liu S (2004) Are variants in the CAPN10 gene related to risk of type 2 diabetes? A quantitative assessment of population and family-based association studies. Am J Hum Genet 74:208–222

Weedon MN, Schwarz PE, Horikawa Y, Iwasaki N, Illig T, Holle R, Rathmann W, Selisko T, Schulze J, Owen KR, Evans J, Del Bosque-Plata L, Hitman G, Walker M, Levy JC, Sampson M, Bell GI, McCarthy MI, Hattersley AT, Frayling TM (2003) Meta-analysis and a large association study confirm a role for calpain-10 variation in type 2 diabetes susceptibility. Am J Hum Genet 73:1208–1212

European Journal of Endocrinology (2005) 153 167–176 ISSN 0804-4643

EXPERIMENTAL STUDY

Endoplasmic reticulum stress induces *Wfs1* gene expression in pancreatic β-cells via transcriptional activation

Kohei Ueda[1], June Kawano[2], Komei Takeda[3], Toshiaki Yujiri[3], Katsuya Tanabe[3], Takatoshi Anno[3], Masaru Akiyama[3], Junichi Nozaki[4], Takeo Yoshinaga[4], Akio Koizumi[4], Koh Shinoda[2], Yoshitomo Oka[5] and Yukio Tanizawa[3]

[1]*Health Service Center, Organization for University Education, Yamaguchi University,* [2]*Division of Neuroanatomy, Department of Neuroscience, and* [3]*Division of Molecular Analysis of Human Disorders, Department of Bio-Signal Analysis, Yamaguchi University Graduate School of Medicine, 1-1-1 Minami Kogushi, Ube, Yamaguchi 755-8505, Japan,* [4]*Department of Health and Environmental Sciences, Kyoto University Graduate School of Medicine, Kyoto, Japan, and* [5]*Division of Molecular Metabolism and Diabetes, Department of Internal Medicine, Tohoku University Graduate School of Medicine, Sendai, Japan*

(Correspondence should be addressed to Y Tanizawa; Email: tanizawa@yamaguchi-u.ac.jp)

Abstract

Objective: The *WFS1* gene encodes an endoplasmic reticulum (ER) membrane-embedded protein. Homozygous *WFS1* gene mutations cause Wolfram syndrome, characterized by insulin-deficient diabetes mellitus and optic atropy. Pancreatic β-cells are selectively lost from the patient's islets. ER localization suggests that WFS1 protein has physiological functions in membrane trafficking, secretion, processing and/or regulation of ER calcium homeostasis. Disturbances or overloading of these functions induces ER stress responses, including apoptosis. We speculated that WFS1 protein might be involved in these ER stress responses.

Design and methods: Islet expression of the Wfs1 protein was analyzed immunohistochemically. Induction of Wfs1 upon ER stress was examined by Northern and Western blot analyses using three different models: human skin fibroblasts, mouse pancreatic β-cell-derived MIN6 cells, and Akita mouse-derived *Ins2* $^{96Y/Y}$ insulinoma cells. The human *WFS1* gene promoter-luciferase reporter analysis was also conducted.

Result: Islet β-cells were the major site of *Wfs1* expression. This expression was also found in δ-cells, but not in α-cells. *WFS1* expression was transcriptionally up-regulated by ER stress-inducing chemical insults. Treatment of fibroblasts and MIN6 cells with thapsigargin or tunicamycin increased *WFS1* mRNA. WFS1 protein also increased in response to thapsigargin treatment in these cells. *WFS1* gene expression was also increased in *Ins2* $^{96Y/Y}$ insulinoma cells. In these cells, ER stress was intrinsically induced by mutant insulin expression. The *WFS1* gene promoter-luciferase reporter system revealed that the human *WFS1* promoter was activated by chemically induced ER stress in MIN6 cells, and that the promoter was more active in *Ins2* $^{96Y/Y}$ cells than *Ins2* $^{wild/wild}$ cells.

Conclusion: *Wfs1* expression, which is localized to β- and δ-cells in pancreatic islets, increases in response to ER stress, suggesting a functional link between *Wfs1* and ER stress.

European Journal of Endocrinology **153** 167–176

Introduction

Wolfram syndrome is a rare recessively inherited genetic disorder, which is characteristically associated with juvenile onset diabetes mellitus and progressive optic atropy (1). Sensorineural deafness, diabetes insipidus, ataxia, urinary-tract atony, peripheral neuropathy and psychiatric illness may also be present (2). We and another group succeeded in cloning the gene responsible for this disorder and designated it *WFS1* (3) or *wolframin* (4). Loss-of-function mutations in the *WFS1* gene have been linked to Wolfram syndrome. The *WFS1* gene consists of eight exons coding for a putative 890 amino acid protein with an apparent molecular mass of ~100 kDa. WFS1 protein (wolframin) is a hydrophobic protein with nine transmembrane segments and large hydrophilic regions at both termini. WFS1 protein localizes primarily to the endoplasmic reticulum (ER) in a N_{cyt}/C_{lum} membrane topology (5, 6). A recent report suggested that expression of WFS1 protein in oocytes was associated with an increase in cytosolic Ca^{2+} and induced novel cation-selective channel activities in the ER membrane (7). However, its role in cellular functions and the mechanism by which mutations of this gene cause Wolfram syndrome remain largely unknown.

DOI: 10.1530/eje.1.01945
Online version via www.eje-online.org

ER is a specialized organella involved in a wide variety of cellular functions. Calcium regulation and post-translational modification, folding and trafficking of secreted and membrane integral proteins are well-defined ER functions (8). Various physiological and pathological conditions interfere with these functions, and overloading of these functions induces ER stress. Cells respond to such stress by activating several adaptive pathways including chaperone induction, protein translation attenuation, and occasionally apoptosis, collectively called the unfolded protein response (9). Characteristically, pancreatic β-cells have highly developed ER apparently due to the heavy demands of insulin biosynthesis and secretion. Beta-cells are highly susceptible to ER stress. Several studies have shown that β-cell mass is reduced in patients with type 2 diabetes, possibly due to apoptotic death of β-cells and to reduced cell proliferation (10). ER stress may be involved in this process (11). In the Akita mouse, an animal model of MODY (maturity onset diabetes of the young), which carries a conformation-altering missense mutation (Cys96Tyr) in the insulin-2 (*Ins2*) gene (12, 13), hyperglycemia and reduced β-cell mass are accompanied by ER stress-induced β-cell death (14). Based on the ER localization of WFS1 protein, it is reasonable to speculate that WFS1 protein may play an as yet undefined role in the ER stress-induced cell death of pancreatic β-cells. In fact, we showed islet cells lacking Wfs1 to be more susceptible to ER stress-induced apoptosis (15), and, more recently, Yamaguchi *et al.* reported that treatment with ER stress inducers increased Wfs1 protein expression in isolated mouse pancreatic islets (16).

In the present study, immunohistochemical staining confirmed β-cells to be the major site of *Wfs1* expression in the mouse pancreas. Furthermore, this expression was also evident in δ-cells but not in α-cells. The *WFS1* gene was clearly expressed in response to drug-induced ER stress in both fibroblasts and pancreatic β-cell-derived MIN6 cells. Under the same conditions, the human *WFS1* promoter luciferase reporter was activated suggesting transcriptional control of *WFS1* expression. Furthermore, *Wfs1* mRNA and protein levels were increased in Akita mouse-derived *Ins2* $^{96Y/Y}$ insulinoma cells, in which the ER stress response had been triggered (17). Our results demonstrate that not only drug-induced but also intrinsic ER stress leads to *WFS1* expression in pancreatic β-cells, and this occurs, at least in part, via transcriptional activation of the *WFS1* promoter. These findings further suggest a functional link between *WFS1* and ER stress responses.

Research design and methods

Tissue preparation and immunohistochemical staining of the mouse pancreas

All experimental protocols for this study were approved by the committee on the Ethics of Animal Experimentation at Yamaguchi University School of Medicine. The anti-Wfs1 antibodies were described previously (5, 15).

Double immunofluorescent staining was performed for co-localization studies. Sections were pre-incubated, bleached (18), and stained with a mixture of anti-Wfs1n (diluted 1:200) and mouse monoclonal anti-insulin (diluted 1:100; Santa Cruz Biotechnology, Santa Cruz, CA, USA), anti-glucagon (diluted 1:200; Sigma-Aldrich, St Louis, MO, USA), or anti-somatostatin (diluted 1:25; Biomeda Corporation, Foster City, CA, USA) in 0.1 M sodium phosphate buffer containing 0.3% Triton X-100, 0.1% sodium azide, and 3% normal goat serum (PBT-NGS) for 24 h at 20 °C. Next, the sections were incubated with a mixture of two secondary antibodies in PBT-NGS for 24 h at 20 °C. The secondary antibodies used were Alexa Fluor 488 conjugated with goat anti-rabbit IgG (H + L), highly cross absorbed (Molecular Probes, Eugene, OR, USA) and diluted 1:100, and an Alexa Fluor 594 conjugated to goat anti-mouse IgG (H + L), F(ab')2 fragment (Molecular Probes), diluted 1:100. The sections were coverslipped with VECTASHIELD mounting medium (Vector Laboratories, Burlingame, CA, USA). As a control, one of the two primary antibodies, for example either anti-Wfs1n or anti-insulin, was removed to check for cross-reactivity. In these control experiments, other procedures were the same as for Wfs1/insulin double staining. No cross-reactivity was observed in these experiments (data not shown).

In the case of double immunostaining for Wfs1 and pancreatic polypeptide (PP) detection, a mixture of anti-Wfs1n (diluted 1:200) and anti-PP (diluted 1:200; Linco Research, St Charles, MO, USA) was used for the primary antibody reaction. In the secondary antibody reaction step, sections were incubated in a mixture of Alexa Fluor 488 conjugated with donkey anti-rabbit IgG (H + L; Molecular Probes) diluted 1:100 and Alexa Fluor 594 conjugated to goat anti-guinea pig IgG (H + L), highly cross absorbed (Molecular Probes) and diluted 1:100 in PBT-NGS containing 3% normal donkey serum. Other procedures for Wfs1/PP double staining were the same as for Wfs1/insulin double staining.

Cell culture and reagents

The mouse insulinoma cell line, MIN6 (19), was a gift from Dr Junichi Miyazaki, Osaka University, Japan. Insulinoma cells derived from the Akita mouse and from normal littermates, *Ins2* $^{96Y/Y}$ cells and *Ins2* $^{WT/WT}$ cells respectively, were described previously (17). These cells were maintained in Dulbecco's modified Eagle's medium (DMEM) (Sigma) supplemented with 15% fetal calf serum in an atmosphere of 5% CO_2 at 37 °C. The genotype for the insulin-2 gene was confirmed by restriction fragment length polymorphism (RFLP), as previously described (12, 13). Human skin fibroblasts

(CCD-1059SK) were obtained from ATCC (Manassas, VA, USA). Thapsigargin, ionomycin, A23187, cyclopiazonic acid, 4-chloro-*m*-cresol, tunicamycin and brefeldin A were purchased from Sigma.

Northern blot analysis

Total RNA isolated using an ISOGEN kit (NIPPON GENE, Tokyo, Japan) was electrophoresed in 1% agarose formaldehyde gel and transferred to nylon filters (Hybond-N plus, Amersham Pharmacia Biotech). The filters were prehybridized and hybridized in a buffer containing 50% deionized formamide, 5 × sodium chloride-sodium phosphate-EDTA buffer (750 mmol/l NaCl, 43.25 mmol/l NaH_2PO_4, 6.25 mmol/l EDTA), 2 × Denhardt's solution (0.04% bovine serum albumin, 0.04% Ficoll, 0.04% polyvinylpyrrolidone), and 0.1% soduim dodecyl sulfate at 42 °C. The hybridization buffer contained a radio-labeled 3.0 kb fragment of mouse *Wfs1* cDNA (GeneBank Accession No. BC046988). After a stringent wash with 0.2 × sodium chloride-sodium citrate buffer (3.3 mmol/l Na-citrate, 3.3 mmol/l NaCl) and 0.1% SDS at 50 °C, autoradiographs were digitally scanned and quantified using FULA2000 (Fuji Film, Tokyo, Japan). The blots were stripped and re-proved with a 1122 bp fragment encompassing the entire coding region of the mouse glyceraldehyde-3-phosphate dehydrogenase (GAPDH) cDNA. The cDNA probes were labeled with a random primer DNA labeling kit (Ready-To-Go DNA Labeling Beads, Amersham Pharmacia Biotech) using α-[^{32}P]deoxy-CTP (Amersham Pharmacia Biotech).

Immunoblotting analysis

Cells were lysed in 20 mmol/l Tris–HCl (pH 7.6), 0.5% Nonidet P-40, 250 mmol/l sodium chloride, 3 mmol/l EDTA, 3 mmol/l EGTA, 1 mmol/l phenylmethylsulfonyl fluoride, 2 mmol/l sodium orthovanadate, 20 μg/ml aprotinin, 1 mmol/l dithiothreitol and 5 μg/ml leupeptin. Proteins in cell lysates were separated in 10% SDS-PAGE gel and then electrophoretically transferred onto a nitrocellulose membrane. All membranes were stained with Ponceau S to confirm equal protein loading. The membrane was blocked with 5% milk in TBS-T (50 mmol/l Tris–HCl, 300 mmol/l NaCl, pH 7.6, 0.1% Tween 20) for 1 h. SDS-PAGE and immunoblotting were carried out as described previously (20). Anti-Bip (GRP74), anti-Chop, anti-phosphorylated eIF2-α, and anti-poly(ADP-ribose) polymerase (PARP) antibodies were purchased from Santa Cruz Biotechnology. Detection was performed using the ECL system (Amersham Pharmacia Biotech).

Luciferase assay

To construct the *WFS1* promoter-luciferase reporter gene, the promoter region of the human *WFS1* gene (−3000 to +20, Genbank Accession No. AC004689) was PCR-amplified from human genomic DNA. The fragment was inserted upstream from the luciferase cDNA in a pGL3-Basic vector (Promega, Madison, WI, USA). A plasmid, pCMVβ (Clontech, Palo Alto, CA, USA), containing the cytomegalovirus (CMV) promoter-driven β-galactosidase gene was used as an internal control for the normalization of transfection efficiency. One day before transfection, MIN6 cells or *Ins2* $^{96Y/Y}$ cells were plated at 1×10^5/well into 6-well tissue culture plates. The reporter plasmid (0.5 μg) and the pCMVβ (0.5 μg) were co-transfected into MIN6 cells or *Ins2* $^{96Y/Y}$ cells in 6-well tissue culture plates using 10 μl LipofectAMINE 2000 (Invitrogen) in serum-free Opti-MEM medium (Invitrogen). Twenty-four hours after transfection, the medium was changed to DMEM containing 15% fetal calf serum and 20 mmol/l glucose, and cultured for a further 24 h. After this 24-h incubation, MIN6 cells were treated with thapsigargin or tunicamycin for an additional 6 h. Cell extracts were prepared, and luciferase and β-galactosidase activities were determined using a β-galactosidase enzyme assay system according to the manufacturer's protocol (Promega).

Results

Wfs1 *expression in the mouse pancreatic islet*

Using immunohistochemistry, it was demonstrated that mouse Wfs1 protein was widely expressed in pancreatic islets except in some peripheral areas, while no signals for Wfs1 protein were detected in exocrine acinar cells (Figs 1 and 2 and data not shown). Using double-immunofluorescent staining, the majority of Wfs1-immunoreactive cells were found to coincide with insulin-producing β-cells. Some minor part of the Wfs1 immunoreactivity was, however, localized to non-β-cells seen in the islet periphery (Fig. 1A–F). Such Wfs1-immunoreactive non-β-cells were found to correspond to somatostatin-producing δ-cells (Fig. 1G–L). There was little difference in Wfs1-immunoreactive intensity between the two endocrine cell types (Fig. 1). Wfs1-immunoreactivity was not evident in glucagon-producing α-cells or in pancreatic polypeptide cells (PP-cells; Fig. 2).

ER stress induces WFS1 *expression in fibroblasts*

ER stress induces cellular responses, collectively termed the unfolded protein response, affecting diverse areas of cellular function such as gene expression, metabolism, cell signaling and apoptosis. Certain reagents are known to disturb ER calcium homeostasis or to inhibit post-translational processing or sorting, and thereby to cause ER stress (9). Chemical insults inducing ER stress, the calcium ionophor A23187 and ionomycin,

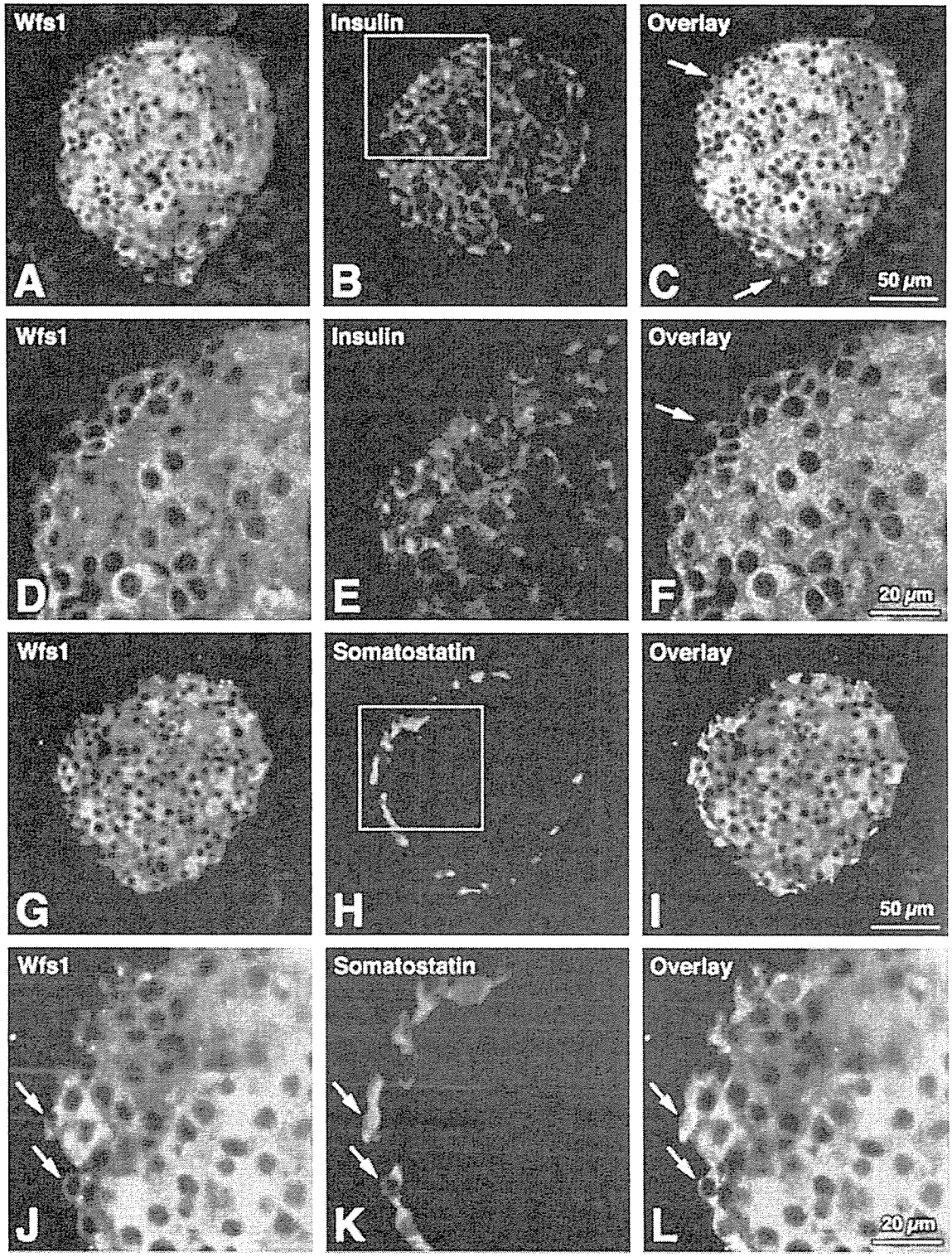

Figure 1 Mouse Wfs1 protein, insulin and somatostatin expression in mouse pancreatic islets. Double immunostaining for mouse Wfs1 (Wfs1: A, D, G, J; Alexa Fluor 488 label; green) and pancreatic hormones (insulin: B, E; somatostatin: H, K; Alexa Fluor 594 label; red) was performed. Panels C, F, I and L are overlaid images. All fluorescent photomicrographs were taken with a confocal microscope LSM 510 (Carl Zeiss Jena GmbH, Jena, Germany). The approximate positions of E and K are indicated by the rectangular frames in B and H respectively. Small solid arrows in C and F indicate non-β endocrine cells immunoreactive for Wfs1. Small solid arrows in J, K and L show somatostatin-producing δ-cells strongly immunoreactive for Wfs1. Note that insulin-producing β-cells and somatostatin-producing δ-cells display Wfs1 immunoreactivity. Scale bars = 50 μm in C and I for A, B, and for G, H; 20 μm in F and L for D, E, and for J, K.

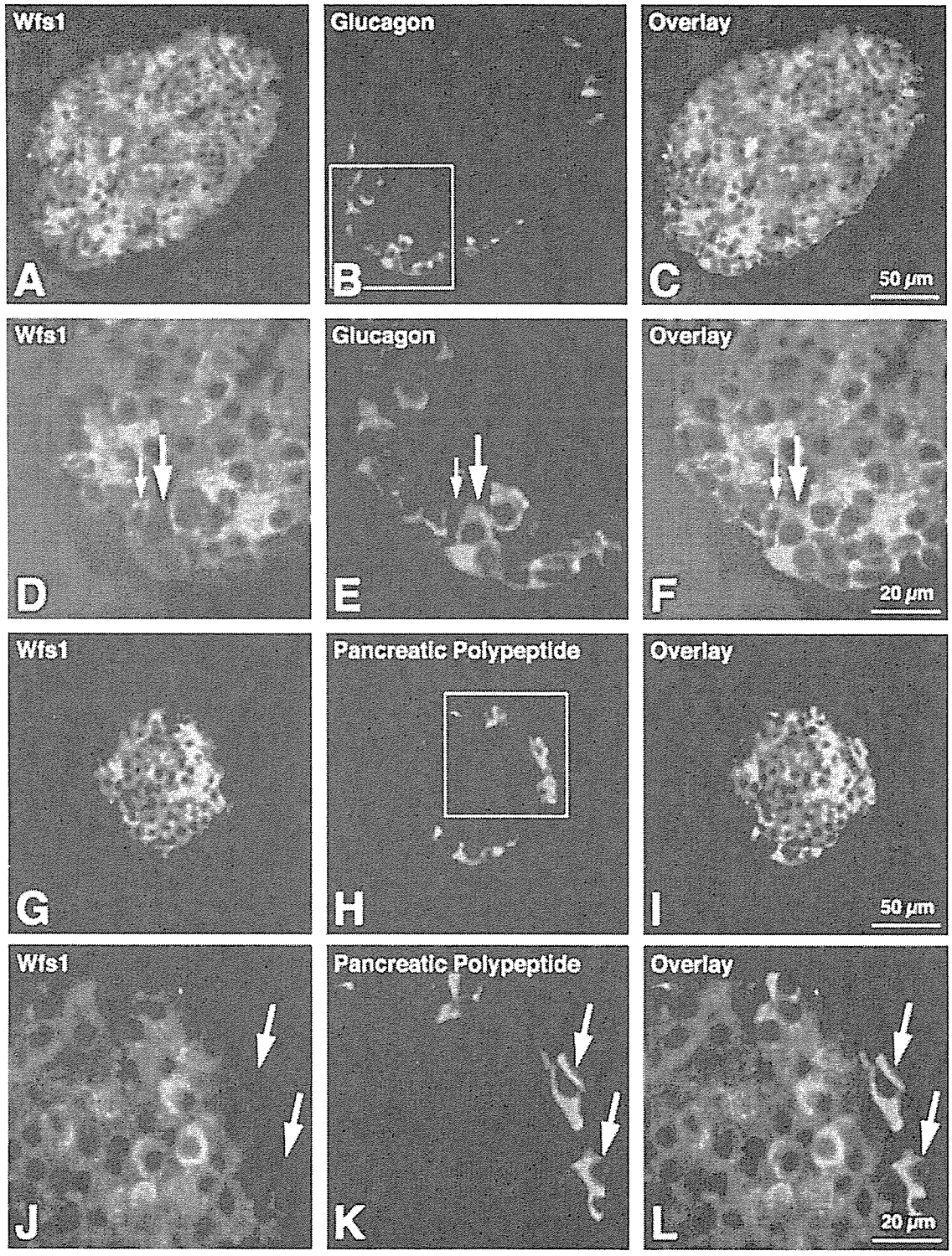

Figure 2 Mouse Wfs1 protein, glucagon and pancreatic polypeptide expression in mouse pancreatic islets. Double immunostaining for mouse Wfs1 (Wfs1: A, D, G, J; Alexa Fluor 488 label; green) and pancreatic hormones (glucagon: B, E; pancreatic polypeptide: H, K; Alexa Fluor 594 label; red) was performed. Panels C, F, I and L are overlaid images. All fluorescent photomicrographs were taken with a confocal microscope LSM 510 (Carl Zeiss Jena GmbH). The approximate positions of E and K are indicated by the rectangular frames in B and H respectively. Large and small solid arrows in D, E and F indicate glucagon-producing α-cells negative for Wfs1 immunoreactivity and non-α endocrine cells positive for Wfs1 immunoreactivity respectively. Large solid arrows in J, K and L show pancreatic polypeptide cells (PP-cells) negative for Wfs1 immunoreactivity. Scale bars = 50 μm in C and I for A, B, and for G, H; 20 μm in F and L for D, E, and for J, K.